Dynamics of a fish-killing dinoflagellate Karenia mikimotoi red-tide captured by composite data sources

Dynamics of a fish-killing dinoflagellate *Karenia mikimotoi* red-tide captured by composite data sources

Kazuhiro Aoki[a,*], Koichi Sugimatsu[b], Naoaki Yoshimura[c], Yoshiyuki Kuroki[d], Hiroki Nakashima[e], Keisuke Hoshina[f], Keisuke Ura[g]

[a]*Fisheries Resources Institute, Fisheries Research and Education Agency, 2-12-4 Fukuura, Kanazawa, Yokohama, Kanagawa 236-8648, Japan*

[b]*Fisheries Technology Institute, Fisheries Research and Education Agency, 1551-8 Taira-machi, Nagasaki, Nagasaki 851-2213, Japan*

[c]*Kumamoto Prefectural Fisheries Research Center, 2450-2 Naka, Oyano-machi, Kami-amakusa, Kumamoto 869-3603, Japan*

[d]*Kumamoto Prefectural Fisheries Development Division, 6-18-1 Suizenji, Chuo-ku, Kumamoto, Kumamoto 862-8570, Japan*

[e]*Kagoshima Prefectural Fisheries Technology and Development Center, 160-10 Aza Takadaue, Iwamoto, Ibusuki-shi, Kagoshima 891-0315, Japan*

[f]*Kagoshima Prefectural Government Fisheries Promotion Division, 10-1 Kamoike-shinmachi, Kagoshima, Kagoshima 890-8577, Japan*

[g]*Azuma-cho Fishery Cooperative Association, 1769-1 Takanosu, Nagashima-cho, Izumi-gun, Kagoshima 899-1401, Japan*

*Corresponding author. Tel. & Fax: +81 45 788 7904

E-mail address: aoki_kazuhiro08@fra.go.jp (Kazuhiro Aoki).

Abstract

Bloom dynamics of *K. mikimotoi* during summer 2015 in the Yatsushiro Sea, Japan, which caused fish mortality was studied using field survey data and satellite data. The bloom initially formed in the western area, subsequently appeared in the southern area, and finally expanded to the central area. The field-survey detected the horizontal displacement of the bloom which was also assessed by satellite data. Acoustic backscattering intensity of the current meter captured the modulation of the diurnal vertical migration of *K. mikimotoi*. After the modulation, *K. mikimotoi* distributed at a shallower depth in the nighttime than the period prior to the modulation. Factors affecting the modulation are suggested to be the continuous low nutrient conditions. Synchronization between the shallowed distribution during the nighttime and the wind driven surface northeastward current enabled a sudden horizontal transport toward the central area. Satellite and acoustic backscattering data are beneficial subsidiary tools for detecting blooms.

Keywords: Karenia mikimotoi, diurnal vertical migration, GOCI, DIN, backscattering intensity

1. Introduction

Harmful algal blooms have frequently occurred and lead to negative influences on human activity in coastal waters characterized by being shallow and adjacent to land (Kudela et al., 2018). Indeed, blooms of the dinoflagellate *Karenia* species particularly have negatively impacts on the economic activities in coastal waters such as *K. brevis* in the Gulf of Mexico, *K. selliformis* in the Mediterranean and Asian waters and *K. mikimotoi* in the European, African and Asian waters (Stumpf et al., 2003; Davidson et al., 2009; Robin et al., 2013; Feki-Sahnoun et al., 2017; Aoki et al., 2017; Chen et al., 2021; Kuroda et al., 2021). It is noteworthy that physical displacement plays a critical role in *Karenia* bloom dynamics (Miyamura et al., 2005; Soto et al., 2018; Aoki et al., 2019). The drastic horizontal displacement of blooms was occurred by currents in short-term (Aoki et al., 2015; 2019). In the case of the rapid bloom development, mitigation strategies can not be efficiently operated in the short-term, consequently mass fish mortality occurs. Therefore, understanding the short-term dynamics of the bloom is critically important.

K. mikimotoi is adapted to a wide range of temperatures of 4-30 °C and salinities of 9-35 (Gentien, 1998; Li et al., 2019). *K. mikimotoi* is motile and undergoes diurnal vertical migration (DVM) distributing in shallower depths during the daytime and at deeper depths during the nighttime (Koizumi et al., 1996; Li et al., 2019). DVM is inhibited by strong light, nutrient deficiency and strong stratification of the water column in the field (Shikata et al., 2015; Yuasa et al., 2018; Shikata et al., 2020).

Previous studies showed the utility of satellite observations for detecting blooms (Stumpf and Tyler,1988; Ahn et al., 2006; Onitsuka et al., 2010). Satellite data have also enabled the detection of specific harmful species not only to estimate the chlorophyll-a concentration (e.g. Kurekin et al., 2014). Siswanto et al. (2013) suggested the detection method of *K. mikimotoi* blooms using Moderate Resolution Imaging Spectroradiometer (MODIS) in the Seto Inland Sea, Japan, which is located near our study area (Fig. 1).

An acoustic current profiler also can measure the backscattering intensity in the water. Using the backscattering intensity, previous studies have attempted to estimate the suspended sediment concentration, zooplankton biomass and micronekton behavior (Heywood, 1996; Luo et al., 2000; Takikawa et al., 2008). Moreover, diurnal vertical migration of zooplankton could be demonstrated using backscattering intensity data (e.g., Heywood, 1996; Berge et al., 2009). Kim et al. (2012) confirmed the increase of backscattering intensity with an increasing in cell abundance of the bloom causing microalga, *Chattonella antiqua*, by a laboratory experiment. Subsequently in the field, the acoustic method was confirmed to be applicable for *Akashiwo sanguinea* and *Alexandrium affine* (Kim et al., 2019).

The Yatsushiro Sea is a semi-enclosed sea area located in the coastal region of western Japan (Fig. 1). Harmful blooms have recurrently occurred in the Yatsushiro Sea and resulted in mass mortality of cultured fishes in fish farms located in the southern area of the Yatsushiro Sea (Onitsuka et al., 2011; Aoki et al., 2015; Nakajima et al., 2019). In the southern area, salinity is higher than that of the inner part because the Yatsushiro Sea is connected with the East China Sea through two channels located in the southern area (Takikawa et al., 2004). Extensive fish aquaculture is conducted around the islands in the southern area.

A *K. mikimotoi* bloom formed in 2015 summer in the Yatsushiro Sea and killed ca. 8000 cultured immature yellowtails with an approximate value of ca. US$ 100000 (at an exchange rate ¥120 = $1). However, the mechanism of the short-term variation of the bloom which is necessary information for mitigation systems, remains unclear. This study described the short-term dynamics of the *K. mikimotoi* bloom in 2015 and the relationship with hydrostatic condition using data observed by the ship survey. In addition, usage of satellite data and backscattering intensity data enable tracking the horizontal distribution and vertical migration of the *K. mikimotoi* blooms in the field. Sonar data such as backscattering of the current meter has been already observed in many monitoring programs of harmful blooms in various coastal waters. In addition, the satellite data can be used in any coastal waters. However, studies using a combination of satellite and sonar data for detecting blooms remain uncommon.

2. Materials and Methods

2.1. Description of field observations

In order to understand the short-term variation of the bloom, field surveys were conducted by the Kumamoto Prefectural Fisheries Research Center (KPFRC), the Kagoshima Prefectural Fisheries Technology and Development Center, the Azuma-cho Fishery Cooperative Association and the Fisheries Research and Education Agency (FRA). The cell density was counted in the weekly surveys during the pre-bloom period and daily surveys during the bloom. Water samples were collected with a Van-Dorn sampler or Kitahara water sampler at depths of 0, 2, 5, 10 m depth for cell counts. Samples were stored in cooler boxes filled with water until cell counts for preventing a temperature increase and sunlight, and cell counts were partially conducted on the ship and the remaining just after getting off a ship using microscopes.

In order to understand the short-term variation of environmental conditions, vertical profiles of the water temperature and salinity were measured using AAQ-RINKO (JFE Advantec Inc.) and dissolved inorganic nitrogen (DIN) and PO_4-P were measured at 0, 5, 10, 20, 30, 40 and 1 m above the bottom using a Van-Dorn water sampler and autoanalyzer (QuAAtro 39, BL-TEC, Japan) at Stations 1-8 (Fig. 1) by KPFRC. The

Monod coefficient (= $N/(N+K_h)$; N: nutrient density; K_h; a half saturation constant) for DIN and PO_4-P was calculated to examine the nutrient condition for the growth of *K. mikimotoi* in the same manner of Aoki et al. (2017). The half saturation constants for DIN and PO_4-P are 0.78 μM and 0.14 μM, respectively (Yamaguchi, 1994; Shikata et al., 2020). The Monod coefficient less than 0.5 means that nutrient concentration is less than the half saturation constant in the environment. Moreover, the Monod coefficient of DIN is directly comparable to the Monod coefficient of PO_4-P for discussing the limiting nutrient. In this study, the minimum value of the Monod coefficient of DIN and PO_4-P was called for a minimum Monod coefficient.

In order to understand the short-term variation of flow conditions and the vertical profile of *K. mikimotoi*, vertical profiles of the current velocity and backscattering intensity of the water were observed at Station 8 (Fig. 1) using a Nortek Aquadopp Current Profiler Z-cell installed in floating buoys by FRA. Backscattering intensity and current velocity were measured at 1.5-m depth and every 1-m from 3 m to 34 m depth. The amplitude and phase of major 16 tidal components (M_2, S_2, K_1, O_1, N_2, K_2, I_2, P_1, L_2, Sa, Ssa, Mm, MSf, Mf, Q_1, M_1) were estimated using the hourly current velocity data and harmonic analysis. The tidal components of the hourly data were eliminated using estimated amplitudes and phases. Moreover, the detided hourly data was filtered by 5-hour low-pass filter.

2.2 Wind data

Wind speed and direction data were provided by the Japan Meteorological Agency at Minamata (Fig. 1).

2.3 Procedure of satellite data

A detection method of *K. mikimotoi* bloom has been suggested using data of Aqua/MODIS (Siswanto et al., 2013). However, we used the data of the Geostationary Ocean Color Imager (GOCI) of the Communication Ocean and Meteorological Satellite of Korea (Ryu et al., 2012) rather than that of Aqua/MODIS, because sufficient data of Aqua/MODIS could not be obtained during 2015 bloom due to the extensive cloud cover. As every hour data of GOCI during daytime can be used for the eastern Asian area, more extensive data could be obtained during the 2015 *K. mikimotoi* bloom in the Yatsushiro Sea. As the spectral bands of GOCI do not match with Aqua/MODIS, we used the alternative spectral bands of GOCI which are listed in Table 1.

2.4 Estimation of horizontal transport

Horizontal transport distance induced by the current was evaluated using current velocity data at Stn. 8. Considering the DVM of *K. mikimotoi*, daily horizontal transport distance was assumed in two cases. Based on observed results of Koizumi et al. (1996), simplified DVM was assumed in case (a) in which velocity in 5-m depth was used during daytime (5:00-17:00), and 25-m depth during nighttime (0:00-4:00, 18:00-24:00). Based on our result shown in section 3.3, DVM with shallowing of the nighttime distribution was assumed in case (b) in which velocity in 5-m depth was used during daytime (5:00-17:00), and 15-m depth during nighttime (0:00-4:00, 18:00-24:00).

3 Results

3.1. Horizontal evolution of the bloom

Cell density of the *K. mikimotoi* increased to 18000 cells ml^{-1} cells in Kusuura Bay which is a semi-enclosed area located in the western area of the Yatsushiro Sea, meanwhile cell density in the eastern area of Yatsushiro Sea ranged 0-3 cells ml^{-1} on 22

July (Fig. 1 and 2). Higher cell density over 10000 cells ml^{-1} distributed to the area outside Kusuura Bay on 28 July. Then, cell density increased to 5000 cells ml^{-1} also around Nagashima and Shishi Islands on 6 and 11 August. High cell density area drastically changed on 13 August, and part of the bloom reached the central area. The northeastern edge of the bloom moved northeastward over 15 km during 11-13 August. Two days later (15 August), the high cell density water distributed along the shore area of the southeastern coast, while it disappeared around Nagashima Island. The cell density in the Yatsushiro Sea suddenly decreased within 2 days from 15 to 17 August. The bloom declined until 24 August.

During the bloom (6-15 August), high chlorophyll-a concentration over 3 mg m^{-3} was detected also in the northern area of the Yatsushiro Sea by satellite data (Fig. 3). Nevertheless, in the northern area, the *K. mikimotoi* bloom was not detected (lower panels of Fig. 3). These results indicate that the high chlorophyll concentration of the northern area was caused by the bloom of another phytoplankton rather than *K. mikimotoi*. Satellite data demonstrated that *K. mikimotoi* bloom occurred mainly in the central and southwestern area, the same as the field observations (Fig. 2 and 3)

3.2. Temporal changes of the environment

Off Kusuura Bay (Stn. 8), sea surface temperature gradually increased from 24.7 to 27.3 °C during late July-middle August when the bloom occurred (Fig. 4). A thermocline and halocline developed in the same period (Fig. 4 and 5). The thermocline temporarily was weakened in the inner area (Stns. 1-6) on 18 August. In Stn. 8, the sea surface salinity slightly increased from 30.9 to 31.3 during late July-early August, while the 30-m depth salinity suddenly increased from 31.8 to 32.6 during 4-11 August (Fig. 4). High salinity (>32.5) water was not observed on 28 July in the surface waters and occurred from the depth of 20-m to the bottom in the bay mouth (Stn. 7; Fig. 5). Subsequently, the high salinity water intruded to the bottom of Stn. 8 on 11 August and Stn. 6 on 18 August (Fig. 4 and 5).

The low surface nutrients and high bottom nutrients were observed from early to mid-July on St. 8 with the stable density stratification (Fig. 4). During mid-July-early August, nutrients in the depth of 20-30 m and Monod coefficient gradually decreased (Fig. 4 and 6). On 28 July and 4 August, minimum Monod coefficient (Monod coefficient of PO_4-P) was less 0.5 in the depth of 20-30 m. On 11 August, Monod coefficient of DIN decreased to ca. 0.5 at sea surface, while the Monod coefficient of PO_4-P increased in synchrony with bottom salinity increased (Fig. 4 and 6). In the results, Monod coefficient of PO_4-P exceeded that of DIN on 11 August. The results indicated the limiting nutrient for the growth of *K. mikimotoi* temporally changed from phosphate to nitrogen on 11 August. Therefore, the minimum Monod coefficient of less 0.6 was maintained until 11 August regardless of the PO_4-P increasing on 11 August.

In early August when the bloom occurred also in Nagashima and Shishi islands (Fig. 2), a southwestward current was observed in the depth shallower than 10-m at Stn. 8 (Fig. 1 and 7). Meanwhile a northeastward current was observed at the depth deeper than 20-m forming a typical two-layer flow pattern of a stratified estuary. The flow pattern apparently changed during 11-12 August when the bloom expanded eastward, and a northeastward current (> 0.05 m s^{-1}) occurred in the depth shallower than 20-m at Stn. 8 which synchronized with a strong northwestward-northward wind (Fig. 7a-c).

3.3 Backscattering intensity of current profilers

Clear diurnal variability was observed in the hourly composite of the backscattering anomaly during the bloom (6-13 August) at Stn. 8 (Fig. 8a). The intensified backscatter was found in the depth shallower than 3-m during daytime and in the depth deeper than 5-m during nighttime.

Interestingly, the backscattering intensity captured a remarkable nighttime vertical distribution in the later stage of the bloom when the bloom expanded to the central area (Fig. 8b). The intensified backscatter was distributed also in the depth deeper than 20-m at nighttime from 6-9 and 12-14 August. The depth of the high backscattering intensity at nighttime was 6-18 m on 10 August and gradually became shallower from 10 to 12 August.

3.4 Horizontal transport

During 28 July-14 August, the direction of transport was mainly to the north to northeast in both cases of a and b (Fig. 7d and e). The difference between case a and b is clearly visible on 12 August. In case (b), highlighted northeastward transport over 7.5 km occurred on 12 August, but not in case (a). Summation of the transport distances in 11-13 August, when the northeastward bloom expansion occurred (Fig. 2), was ca. 6.6 km in case (a) and ca. 11.8 km in case (b), respectively.

4 Discussion

The *K. mikimotoi* bloom initially occurred in a semi-enclosed area of the southwestern area during the summer of 2015 (Fig. 2). Subsequently, the bloom occurred also around the islands in the southern area in early August, and central area in mid-August. In the field survey, bloom transition remained unclear in the northern area during 11-13 August. Satellite observations showed no indication of the bloom occurrence in the northern area in the period (Fig. 3). Therefore, results of the ship survey showed the possibility of two steps of horizontal transport of the bloom. One is transport from

Kusuura Bay to the vicinity area around the islands in the southern area during 28 July-6 August. The other is the transport from the vicinity of the area around the islands in southern area to the central area during 11-13 August. The direction of the horizontal transport in both cases of (a) and (b) estimated by the observed current velocity data was northeastward from 28 July to 6 August (southwestward; Fig. 7). The estimated direction was entirely different from the displacement of the bloom area (Fig. 2). Thus, our results suggested that the bloom occurrence around the islands in the southern area on 6 August resulted from local growth of *K. mikimotoi* in the area rather than transport by the currents. Meanwhile, the direction of the estimated transport in case (a) assumed the default DVM (5-m depth during daytime and 25-m depth during night) was northeastward the same as the displacement of the bloom area during 11-13 August (Fig. 2 and 7). However, the estimated distance of 6.6-km in the case (a) was underestimated in comparison with the displacement of the bloom (over 15 km). Here, we verified the vertical distribution of *K. mikimotoi* during 11-13 August. The backscattering data of the current meter indicated the DVM pattern during the *K. mikimotoi* bloom and the shallowing in the night distribution of the intensified backscattering (Fig. 8). The diurnal pattern of high backscattering is analogous to the DVM of *K. mikimotoi* reported by previous studies (Koizumi, 1996; Shikata et al., 2015). Thus, the result implies that the intensified backscatter indicates the dominance of *K. mikimotoi* during the bloom rather than zooplankton or fishes. Moreover, the shallowed night distribution of intensified backscattering possibly indicates the shallowing of the *K. mikimotoi* distribution during the night (i.e. modulation of the DVM of *K. mikimotoi*) and at least the absence of the high cell density of *K. mikimotoi* in the lower depth during 11-13 August. Thus, case (a) was inadequate for estimating the transport distance during 11-13 August. The estimated distance of 11.8 km in the case (b) assuming the above shallowed night distribution was slightly underestimated, but not largely different from the displacement of the bloom (Fig. 2 and 7e). Moreover, the direction of the estimated transport in case (b) was northeastward the same as the displacement of the bloom area during 11-13 August (Fig. 2 and 7). Therefore, our results implied that the bloom occurring in the central area on 13 August originated from the bloom around the islands in the southern area on 11 August. The displacement of the bloom released aquaculture farms around the islands in the southern area from the stress and damage by the bloom. In fact, the damage of US$ 100,000 during the 2015 *Karenia* bloom was much smaller than the damages (US$ 44,000,000 and 58,000,000) during the blooms in 2009 and 2010 (Aoki et al., 2012; Aoki et al., 2015). One factor of the mitigated damages is the exposure time for the bloom was shortened by the displacement of the bloom.

This study attempted the detection method of the *K. mikimotoi* bloom using GOCI partially differing from Aqua/MODIS (Siswanto et al., 2013). The results were in good agreement with the field survey (Fig. 2 and 3). Therefore, it is suggested that the method of Siswanto et al. (2013) is useful also for GOCI data. As mentioned in section 2.2, GOCI supplies hourly products of a fixed area in East Asian during daytime because of the geostationary orbit. The GOCI data enable measurements of harmful algal blooms even under cloudy conditions. The combination of the method of Siswanto et al. (2013) and hourly products of GOCI will facilitate the detection of *K. mikimotoi* blooms.

The bloom detection method of Siswanto et al. (2013) used remote sensing reflectance of the 6 spectral bands listed in Table 1. The band resolution of the sensor is slightly coarse for resolving the color transition of the ocean which is blue in default state and a reddish brown during the bloom of *K. mikimotoi*. Therefore, it is difficult to develop the method for a more precise measurement of cell density rather than the presence or absence of the bloom. The launch of the satellite installed the high band resolution sensor may enable to detect the cell density of *K. mikimotoi*.

In previous studies, the acoustic detection was confirmed for the bloom of *Chattonella antiqua*, *Akashiwo sanguinea* and *Alexandrium affine* (Kim et al., 2012; Kim et al., 2019) but not for *K. mikimotoi*. As the cell size of *K. mikimotoi* is not much smaller than the *C. antiqua* and *A. sanguinea*, acoustic backscattering is expected to capture the cell density of the *K. mikimotoi*.

In the period of the bloom expansion from the southern area to the central area, the night distribution of *K. mikimotoi* was shallowed in comparison with the distribution prior to the expansion (Fig. 8). During the shallowed distribution, a strong northwest-northward wind induced the northeastward current in the depth shallower than 20m (Fig. 7a-c). In case b, *K. mikimotoi* fully received the effect of the northeastward current, long northeastward transport was evaluated same as the measured bloom expansion but not in case a (Fig. 2 and 7d, e). These results indicated that two key factors of the horizontal transport in mid-August are a shallowed night distribution of *K. mikimotoi* and strong wind-induced current.

The continuous low nutrient condition and alternation of the limiting nutrient from P to N occurred prior to the shallowing in the night distribution of *K. mikimotoi* (Fig. 6). Unclear DVM was shown in N-depleted condition and no DVM in P-depleted in a laboratory experiment (Yuasa et al., 2018). In addition, the vertical migration distance of *K. mikimotoi* correlated to P concentration in the field rather than N concentration (Shikata et al., 2020). Therefore, it suggested that the shallowing of the night distribution during 10-12 August was contributed by the continuous low nutrient condition rather than the alternation of limiting nutrient. The nutrient dynamics are difficult to interpret. The high salinity bottom water gradually intruded into the Yatsushiro Sea through the Nagashima Strait from offshore during 4-18 August (Fig. 4 and 5). The high salinity bottom water did not include high PO_4-P in the strait (Stn. 8) on 4 August. In addition, increasing the PO_4-P is clearer in the upper layer (above 20-m) than the lower layer. These results showed no indication of a clear contribution of the intrusion of high salinity bottom water. It is known that a benthic flux of DIN and PO_4-P from the bottom sediment occurs in the coastal sea areas (Callender and Hammond, 1982; Friedrich et al., 2002). On 11 August, DIN decreased on Stn. 8 rather than increased (Fig. 6). There is also no indication of the contribution of the benthic nutrient flux. Therefore, it is assumed that DIN decreasing and PO_4-P increasing were affected by a combination of multiple factors (utilization for the growth, offshore high salinity water intrusion and benthic flux).

For modeling of the horizontal transport of plankton, vertical distribution of the target is critically important as shown in Fig. 7de and previous studies (Stenevik et al., 2003; Lett et al., 2007; Xiong et al., 2022). In the modeling of *K. mikimotoi* blooms in previous studies (Vanhoutte-Brunier et al., 2008; Gillibrand et al., 2016), the rhythm and swimming speed was not taken into account or does not depend on the development stage of the bloom and/or nutrient condition. The problem is possibly included also in the full-fledged pioneering modeling work targeting *Alexandrium fundyense* in the Gulf of Maine (McGillicuddy et al., 2008). DVM of *A. fundyense* was observed in the laboratory and a salt pond, but not in the ocean (Anderson and Stolzenbach, 1985; Macintyre et al., 1997; Townsend et al., 2005). The dynamics of DVM remain unclear even in well-studied harmful algae (e.g., *A. fundyense* and *K. mikimotoi*). The continuous vertical profiling of the chlorophyll fluorescence in the field and laboratory experiments using columnar aquariums are effective tools for clarifying the dynamics (Koizumi et al., 1996; Shikata et al., 2015; Sakaguchi et al., 2017; Yuasa et al., 2018). Finally, it is hoped that clarifying the dynamics of DVM will enable prediction of the development and/or decline of blooms using real-time monitoring data.

5 Conclusion

This study showed that the *Karenia* bloom occurring in Yatsushiro Sea in 2015, which initially developed in the western and southern area, subsequently expanded to the central area. Satellite detection method of *K. mikimotoi* blooms developed by a previous study using Aqua/MODIS could be applied to the bloom in Yatsushiro Sea using GOCI. The satellite detected bloom area matched with the field survey and complemented the field survey. The sudden horizontal displacement of the bloom during mid-August was driven by the wind driven surface northeastward current and modulation of DVM of *K. mikimotoi*. The modulation of DVM was documented by the acoustic backscattering data of the current meter. The modulation possibly resulted from the continuous low nutrient conditions.

Acknowledgments

We express our appreciation to Japan Meteorological Agency for supplying the wind data. We should like to acknowledge the anonymous reviewers and Dr. Tomoyuki Shikata, Fisheries Research and Education Agency, for their useful comments and suggestions on the manuscripts. The research was partly supported by the Fisheries Agency of Japan and Japan Society for the Promotion of Science Kakenhi 21A402.

References

Ahn, Y.H., Shanmugam, P., Ryu, J.H., Jeong, J.C., 2006. Satellite detection of harmful algal bloom occurrences in Korean waters. Harmful Algae 5, 213-231.

Anderson, D.M., Stolzenbach, K.D., 1985. Selective retention of two dinoflagellates in a well-mixed estuarine embayment: the importance of vertical migration and surface avoidance. Marine Ecology Progress Series 25, 39-50.

Aoki, K., Kuroda, H., Setou, T., Okazaki, M., Yamatogi, T., Hirae, S., Ishida, N., Yoshida, K., Mitoya, Y., 2019. Exceptional red-tide of fish-killing dinoflagellate *Karenia mikimotoi* promoted by typhoon-induced upwelling. Estuarine, Coastal and Shelf Science 219, 14-23.

Aoki, K., Kameda, T., Yamatogi, T., Ishida, N., Hirae, S., Kawaguchi, M., Syutou, T., 2017. Spatio-temporal variations in bloom of the red-tide dinoflagellate *Karenia mikimotoi* in Imari Bay, Japan in 2014: Factors controlling horizontal and vertical distribution. Marine Pollution Bulletin 124, 130-138.

Aoki, K., Onitsuka, G., Shimizu, M., Kuroda, H., Matsuo, H., Kitadai, Y., 2015. Interregional differences in mortality of aquacultured yellowtail *Seriola quinqueradiata* in relation to a *Chattonella* bloom in the Yatsushiro Sea, Japan. Fisheries Science, 81, 525-532.

Aoki, K., Onitsuka, G., Shimizu, M., Kuroda, H., Matsuyama, Y., Kimoto, K., Matsuo, H., Kitadai, Y., Sakurada, K., Nishi, H., Tahara, Y., 2012. Factors controlling the spatio-temporal distribution of the 2009 *Chattonella antiqua* bloom in the Yatsushiro Sea, Japan. Estuarine, Coastal and Shelf Science 114, 148-155.

Berge, J., Cottier, F., Last, K.S., Varpe, Ø., Leu, E., Søreide, J., Eiane, K., Falk-Petersen, S., Willis., K., Nygård, H., Vogedes, D., Griffiths, C., Johnsen, G., Lorentzen, D., Brierley, A.S., 2009. Diel vertical migration of Arctic zooplankton during the polar night. Biology Letters 5, 69-72.

Callender, E., Hammond, D.E., 1982. Nutrient exchange across the sediment-water interface in the Potomac River estuary. Estuarine Coastal and Shelf Science 15, 395-413.

Chen, B., Wang, K., Guo, H., Lin, H., 2021. *Karenia mikimotoi* blooms in coastal waters of China from 1998 to 2017. Estuarine, Coastal and Shelf Science 249, 107034.

Davidson, K., Miller, P., Wilding, T.A., Shutler, J., Bresnan, E., Kennington, K., Swan, S., 2009. A large and prolonged bloom of *Karenia mikimotoi* in Scottish waters in 2006. Harmful Algae 8, 349-361.

Feki-Sahnoun, W., Hamza, A., Njah, H., Barraj, N., Mahfoudi, M., Rebai, A., Hassen, A.B., 2017. A Bayesian network approach to determine environmental factors controlling *Karenia selliformis* occurrences and blooms in the Gulf of Gabès, Tunisia. Harmful Algae 63, 119-132.

Friedrich, J., Dinkel, C., Friedl, G., Pimenov, N., Wijsman, J., Gomoiu, M.T., Cociasu, A., Popa, L., Wehrli, B., 2002. Benthic nutrient cycling and diagenetic pathways in the north-western Black Sea. Estuarine, Coastal and Shelf Science 54, 369-383.

Gentien, P., 1998. Bloom dynamics and ecophysiology of the *Gymnodinium mikimotoi* species complex. In: Anderson, D.M., Cembella, A.D., Hallegraeff, G.M. (Eds.), Physiological ecology of harmful algal blooms, Springer-Verlag, Berlin, pp. 95–112.

Gillibrand, P.A., Siemering, B., Miller, P.I., Davidson, K., 2016. Individual-based modeling of the development and transport of a *Karenia mikimotoi* bloom on the North-west European continental shelf. Harmful Algae 53, 118-134.

Heywood, K.J., 1996. Diel vertical migration of zooplankton in the Northeast Atlantic. Journal of Plankton Research 18, 163-184.

Kim, H., Kang, D., Jung, S.W., Kim, M., 2019. High-frequency acoustic backscattering characteristics for acoustic detection of the red tide species *Akashiwo sanguinea* and *Alexandrium affine*. Journal of Oceanology and Limnology 37, 1268-1276.

Kim, J., Choi, J.W., Kang, D., 2012. Laboratory experiment to measure 5-MHz volume backscattering strengths from red-tide causing microalgae *Chattonella antiqua*. Ocean Science Journal 47, 173-179.

Koizumi, Y., Uchida, T., Honjo, T., 1996. Diurnal vertical migration of *Gymnodinium mikimotoi* during a red tide in Hoketsu Bay, Japan. Journal of Plankton Research 18, 289-294.

Kudela, R.M., Raine, R., Pitcher, G.C., Gentien, P., Berdalet, E., Enevoldsen, H., Urban, E., 2018. Establishment, goals and legacy of global ecology and oceanography of harmful algal blooms (GEOHAB) programme. In: Glibert, P.M., Berdalet, E., Burford, M.A., Pitcher, G.C., Zhou, M. (Eds.), Global ecology and oceanography of harmful algal blooms, Springer International Publishing, Cham, pp. 27-49.

Kurekin, A.A., Miller, P.I., Van der Woerd, H.J., 2014. Satellite discrimination of *Karenia mikimotoi* and *Phaeocystis* harmful algal blooms in European coastal waters: Merged classification of ocean colour data. Harmful Algae 31, 163-176.

Kuroda, H., Azumaya, T., Setou, T., Hasegawa, N., 2021. Unprecedented outbreak of harmful algae in Pacific coastal waters off southeast Hokkaido, Japan, during late summer 2021 after record-breaking marine heatwaves. Journal of Marine Science and Engineering 9, 1335.

Lett, C., Veitch, J., Van der Lingen, C.D., Hutchings, L., 2007. Assessment of environmental barrier to transport of ichthyoplankton from the southern to the northern Benguela ecosystems. Marine Ecology Progress Series 347, 247-259.

Li, X., Yan, T., Yu, R., Zhou, M., 2019. A review of *Karenia mikimotoi*: Bloom events, physiology, toxicity and toxic mechanism. Harmful Algae 90, 101702.

Luo, J., Ortner, P.B., Forcucci, D., Cummings, S.R., 2000. Diel vertical migration of zooplankton and mesopelagic fish in the Arabian Sea. Deep Sea Research II 47, 1451-1473.

Macintyre, J.G., Cullen, J.J., Cembella, A.D., 1997. Vertical migration, nutrition and toxicity in the dinoflagellate *Alexandrium tamarense*. Marine Ecology Progress Series

148, 201-216.

Miyamura, K., Mikajiri, T., Kanazawa, K., 2005. Characteristics of a red tide due to the harmful dinoflagellate *Karenia mikimotoi* occurred in Usuki Bay (Japan), Oita prefecture, in 2003. Bulletin of the Japanese Society of Fisheries Oceanography 69, 91-98 (in Japanese).

McGillicuddy, D.J., Anderson, D.M., Stock, C.A., Lynch, D.R., Townsend, D.W., 2008. Modeling blooms of *Alexandrium fundyense* in the Gulf of Maine. In: Babin, M., Roesler, C.S., Cullen, J.J. (Eds) Real-time coastal observing systems for marine ecosystem dynamics and harmful algal blooms: Theory instrumentation and modeling. UNESCO, Paris, pp 599-626.

Nakajima, H., Murata, K., Yano, K., Nishi, H., Yoshimura, N., Kuroki, Y., Kawasaki, S., Furukawa, S., Ura, K., Matsuo, H., Kitatsuji, S., Shikata, T., Abe, K., Tokunaga, T., Okamura, K., Aoki, K., Onitsuka, G., 2019. A *Chattonella* bloom in the Yatsushiro Sea, Japan in summer 2016: Environmental characteristics during the bloom and mortality of cultured yellowtail *Seriola quinqueradiata*. Nippon Suisan Gakkaishi 85, 162-172 (in Japanese and English abstruct).

Onitsuka, G., Miyahara, K., Hirose, N., Watanabe, S., Semura, H., Hori, R., Nishikawa, T., Miyaji, K., Yamaguchi, M., 2010. Large-scale transport of *Cochlodinium polykrikoides* blooms by the Tsushima Warm Current in the southwest Sea of Japan. Harmful Algae 9, 390-397.

Onitsuka, G., Aoki, K., Shimizu, M., Matsuyama, Y., Kimoto, K., Matsuo, H., Kitadai, Y., Nishi, H., Tahara, Y., Sakurada, K., 2011. Short-term dynamics of a *Chattonella antiqua* bloom in the Yatsushiro Sea, Japan, in summer 2010: characteristics of its appearance in the southern area. Bulletin of the Japanese Society of Fisheries Oceanography 75, 143-153 (in Japanese with English abstract).

Robin, R.S., Kanuri, V.V., Muduli, P.R., Mishra, R.K., Jaikumar, M., Karthikeyan, P., Kumar, C.S., Kumar C.S., 2013. Dinoflagellate bloom of *Karenia mikimotoi* along the southeast Arabian Sea, bordering western India. Journal of Ecosystems, doi: 10.1155/2013/463720.

Ryu, J.H., Han, H.J., Cho., S., Park, Y.J., Ahn, Y.H., 2012. Overview of geostationary ocean color imager (GOCI) and GOCI data processing system (GDPS). Ocean Science Journal 47, 223-233.

Sakaguchi, M., Yamatogi, T., Hirae, S., Ishida, N., Hirano, K., Aoki, K., 2017. Diurnal vertical migration of *Chattonella* spp. in mesocosm during a red tide in Isahaya Bay, Nagasaki prefecture, Japan. Bulletin of Plankton Society, Japan 64, 1-10 (in Japanese with English abstract).

Shikata, T., Kitatsuji, S., Abe, K., Onitsuka, G., Matsubara, T., Nakayama, N., Yuasa, K., Nishiyama, Y., Mizuno, K., Masuda, T., Nagai, K., 2020. Vertical distribution of a harmful red-tide dinoflagellate, *Karenia mikimotoi*, at the decline stage of blooms. Journal of Sea Research 165, 101960.

Shikata, T., Sakamoto, S., Onitsuka, G., Aoki, K., Yamaguchi, M., 2015. Effects of salinity on diel vertical migration behavior in two red-tide algae, *Chattonella antiqua* and *Karenia mikimotoi*. Plankton and Benthos Research 9, 42-50.

Siswanto, E., Ishizaka, J., Tripathy, S.C., Miyamura, K., 2013. Detection of harmful algal blooms of *Karenia mikimotoi* using MODIS measurements: A case study of Seto Inland Sea, Japan. Remote Sensing of Environment 129, 185-196.

Soto, I.M., Cambazoglu, M.K., Boyette, A.D., Broussard, K., Sheehan, D., Howden S.D., Shiller, A.M., Dzwonkowski, B., Hoda, L., Fitzpatrick, P.J., Arnone, R.A., Mickle, P.F., Cressman, K., 2018. Advection of *Karenia brevis* blooms from the Florida Panhandle towards Mississippi coastal waters. Harmful Algae 72, 46-64.

Stenevik, E.K., Skogen, M., Sundby, S., Boyer, D., 2003. The effect of vertical and horizontal distribution on retention of sardine (*Sardinops sagax*) larvae in the Northern Benguela: Observation and modelling. Fisheries Oceanography 12, 185-200.

Stumpf, R.P., Culver, M.E., Tester, P.A., Tomlinson, M., Kirkpatrick, G.J., Pederson, B.A., Truby, E., Ransibrahmanakul, V., Soracco, M., 2003. Monitoring *Karenia brevis* blooms in the Gulf of Mexico using satellite ocean color imagery and other data. Harmful Algae 2, 147-160.

Stumpf, R.P., Tyler, M.A., 1988. Satellite detection of bloom and pigment distribution in estuaries. Remote Sensing of Environment 24, 385-404.

Takikawa, K., Tanaka, K., Mori, E., Watanabe, K., Hokamura, T., Aoyama, C., 2004. Factorial analysis of environmental variables over Yatsushiro-Sea. Annual Journal of Coastal Engineering, Japan Society Civil Engineers 51, 916-920. (in Japanese)

Takikawa, T., Kitamura, M., Horimoto, N., 2008. Horizontal current field, ADCP backscatter, and plankton distribution in Sagami Bay, Japan. Fisheries Oceanography 17, 254-262.

Townsend, D.W., Bennett, S.L., Thomas, M.A., 2005. Diel vertical distributions of the red tide dinoflagellate *Alexandrium fundyense* in the Gulf of Maine. Deep-Sea Research II 52, 2593-2602.

Vanhoutte-Brunier, A., Fernand, L., Ménesguen, A., Lyons, S., Gohin, F., Cugier, P., 2008. Modelling the *Karenia mikimotoi* bloom that occurred in the western English Channel during summer 2003. Ecological Modelling 210, 351-376.

Xiong, J., Shen, J., Wang, Q., 2022. Storm-induced coastward expansion of *Margalefidinium polykrikoides* bloom in Chesapeake Bay. Marine Pollution Bulletin 184, 114187.

Yuasa, K., Shikata, T., Kuwahara, Y., Nishiyama, Y., 2018. Adverse effects of strong light and nitrogen deficiency on cell viability, photosynthesis, and motility of the red-tide dinoflagellate *Karenia mikimotoi*. Phycologia 57, 525-533.

Yamaguchi, M., 1994. Physiological ecology of the red tide flagellate *Gymnodinium nagasakiense* (Dinophyceae). Bulletin of Nansei National Fisheries Research Institute 27, 251-394 (in Japanese).

Figure captions

Fig. 1. Map of the study area in Yatsushiro Sea, Japan. Numbered circles and closed square indicate locations of monitoring stations for the vertical profiles of the water quality (Stations 1-8) and meteorological station at Minamata, respectively. At Stn. 8, current velocity and backscattering intensity was observed by floating buoy.

Fig. 2. Spatio-temporal variation of the maximum cell density of the *Karenia mikimotoi* in Yatsushiro Sea during 6 July-24 August 2015.

Fig. 3. Horizontal distribution of the satellite chlorophyll concentration (upper panels) and detected *K. mikimotoi* bloom by GOCI (gray pixels in lower panels) during 6-15 August.

Fig. 4. Hovmoller diagram of temperature, salinity, DIN and PO_4-P at Stn. 8.

Fig. 5. Vertical sections of temperature (left panels) and salinity (right panels) in Yatsushiro Sea during 28 July-18 August.

Fig. 6. Hovmoller diagram of Monod coefficient for DIN (upper panel), PO4-P (middle panel) and minimum Monod coefficient (lower panel) at Stn. 8.

Fig. 7. Hovmoller diagram of eastward velocity(a) and northward velocity (b) at Stn. 8. Time series of wind vectors at Minamata meteorological station (c). Horizontal transport distance of case a (panel d) and b (panel e).

Fig. 8. Hourly composite of the backscattering intensity anomaly (a) and hovmoller diagram of the backscattering intensity anomaly (b) at Stn. 8 during 6-14 August. Black and white bars on both graphs indicate the light-dark cycle.

Table 1. Spectral bands used for detecting the *K. mikimotoi* bloom.

Aqua/MODIS (nm)	GOCI/COMS (nm)
412	412
443	443
488	490
547	555
667	660
678	680

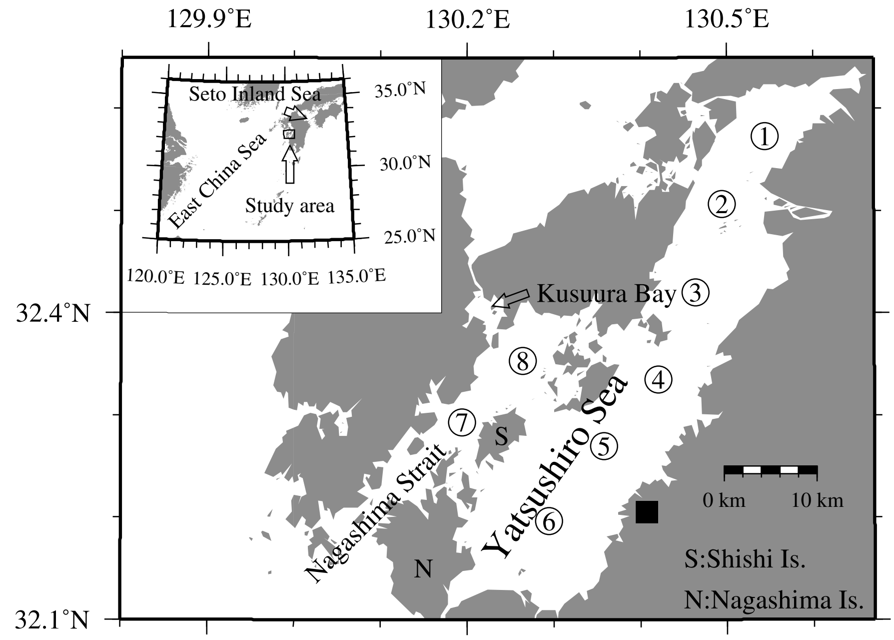

Fig.1 Aoki et al.

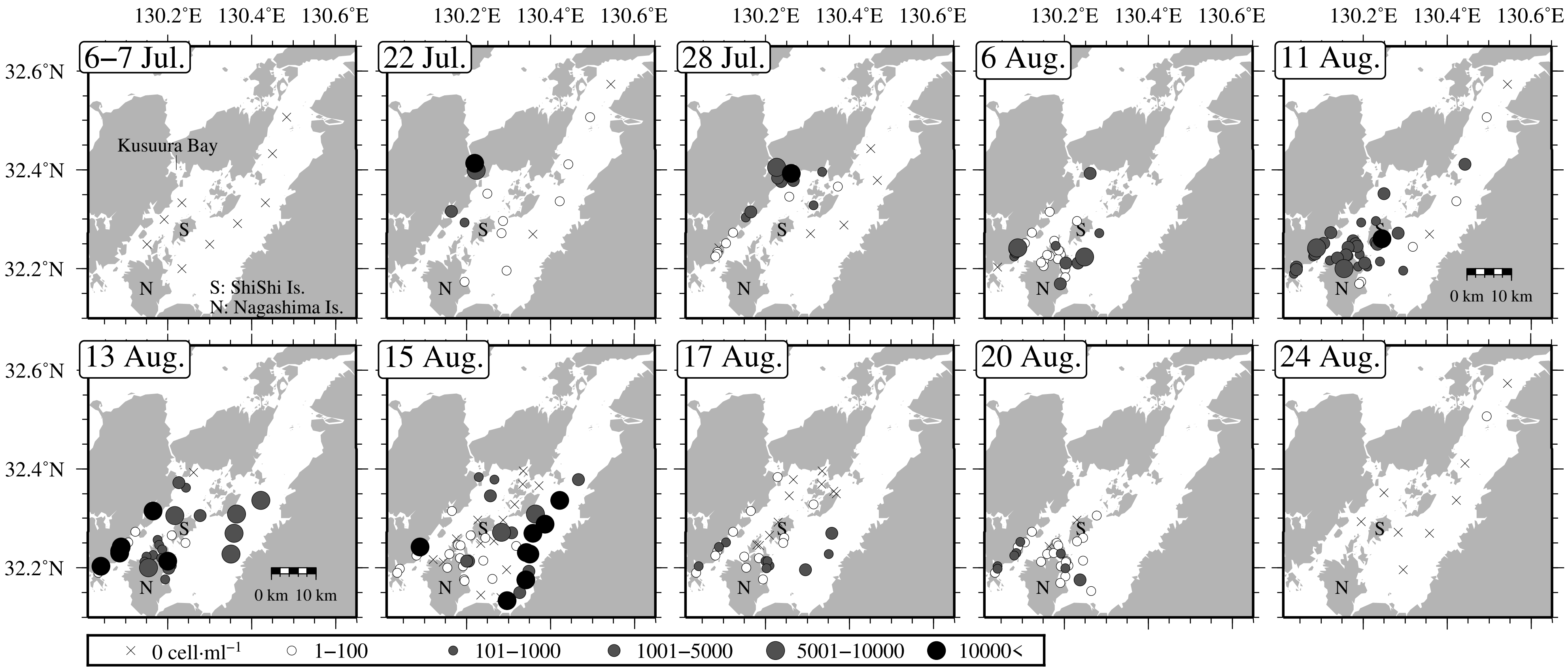

Fig.2 Aoki et al.

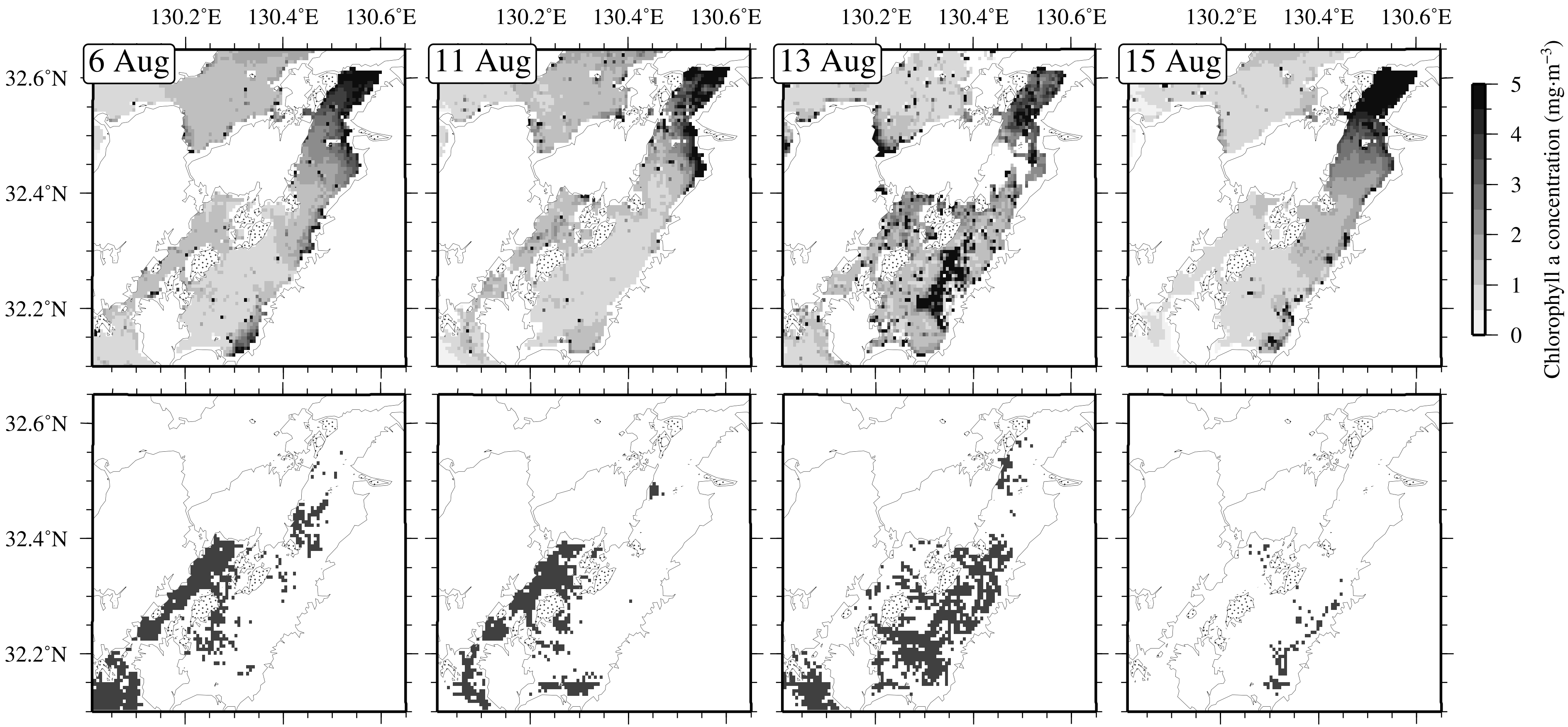

Fig.3 Aoki et al.

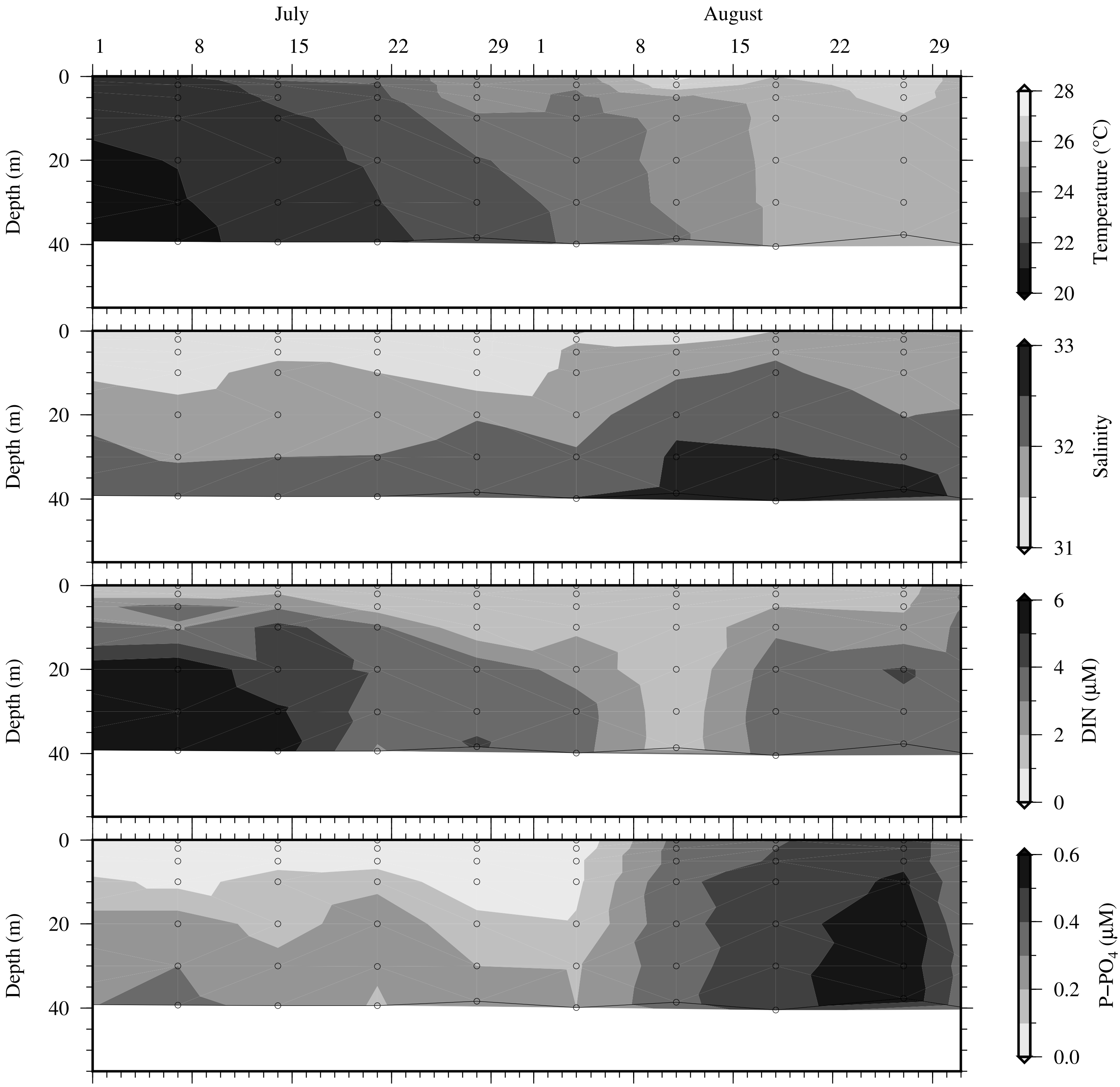

Fig.4 Aoki et al.

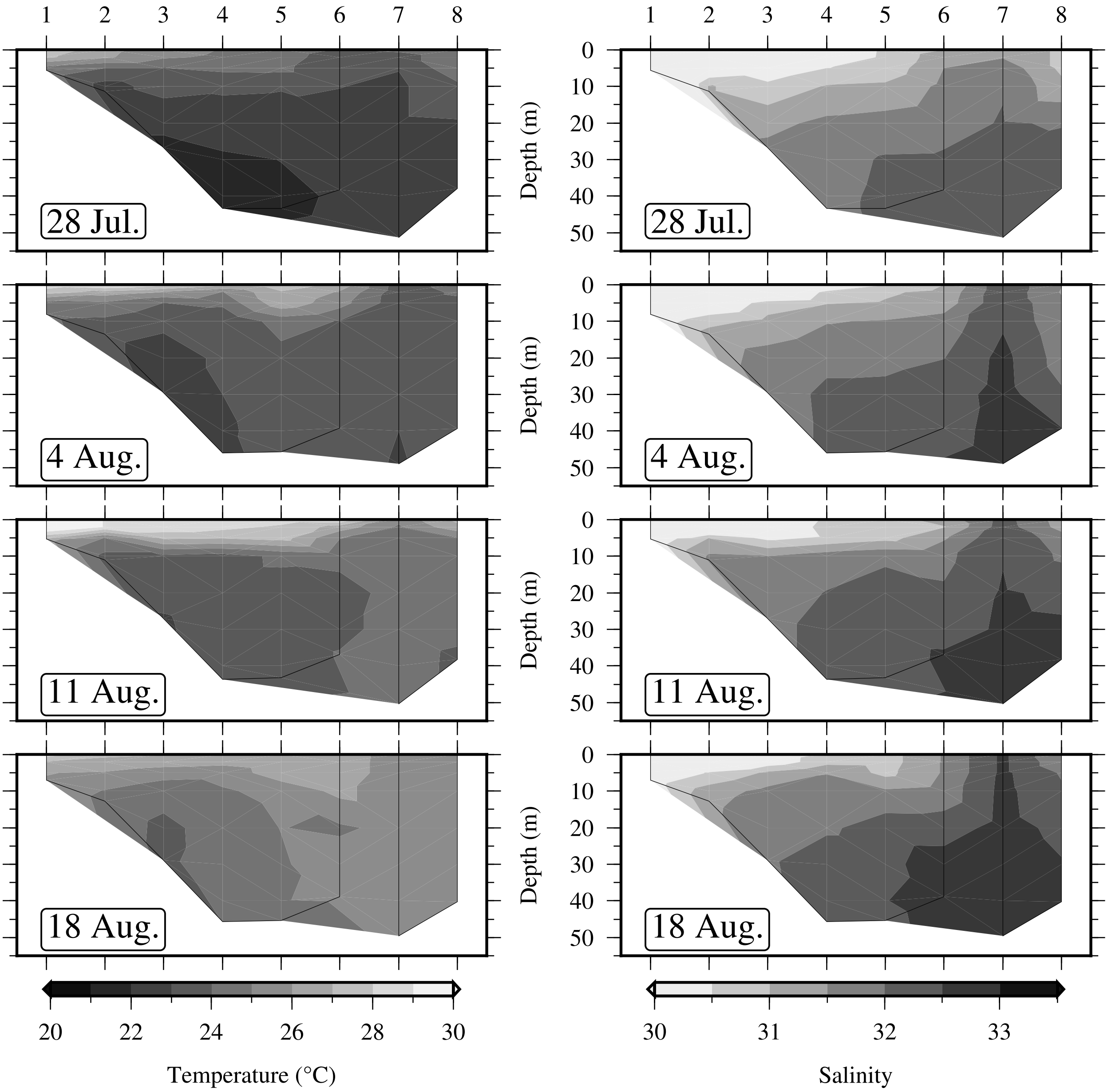

Fig.5 Aoki et al.

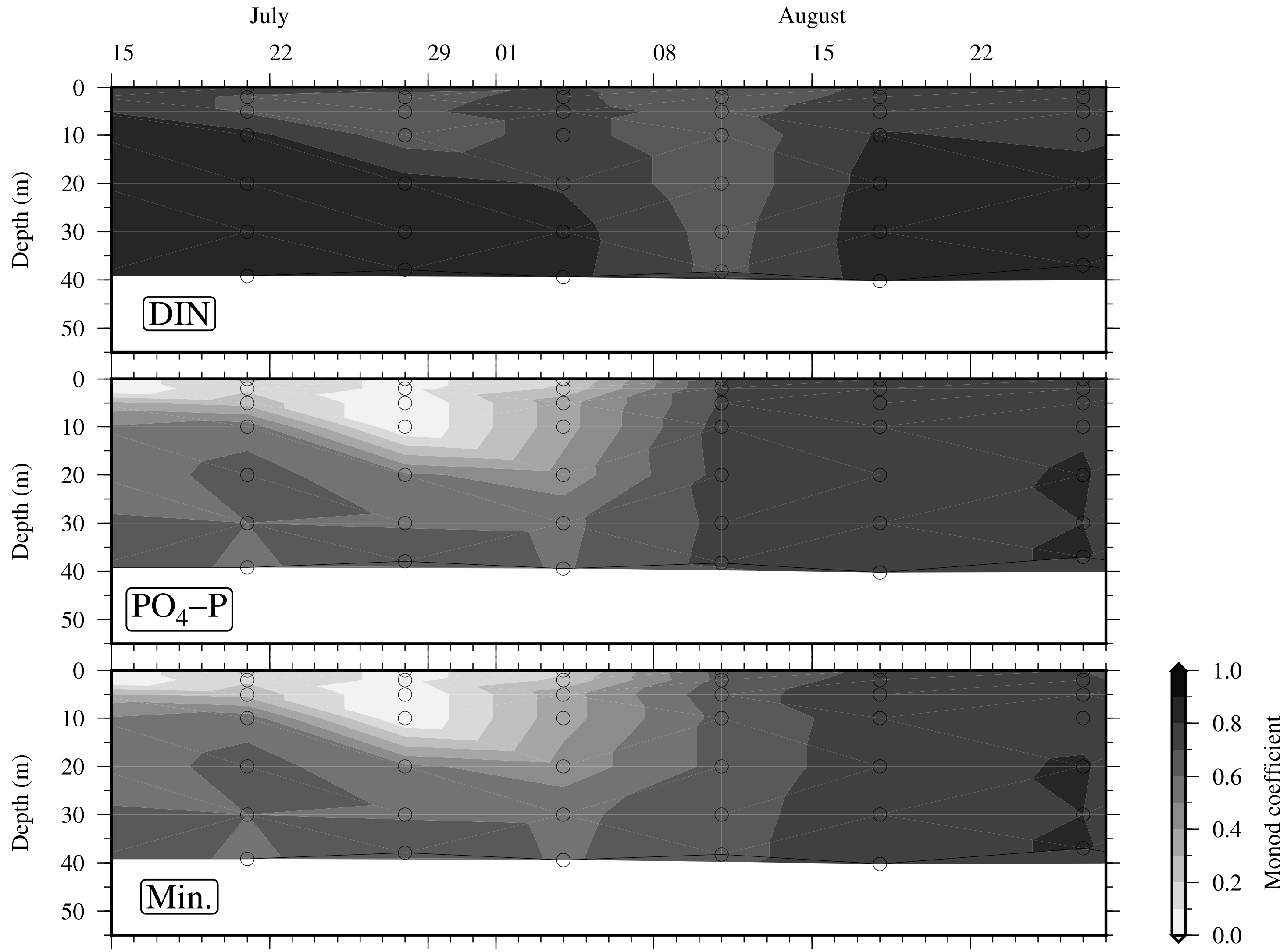

Fig.6 Aoki et al.

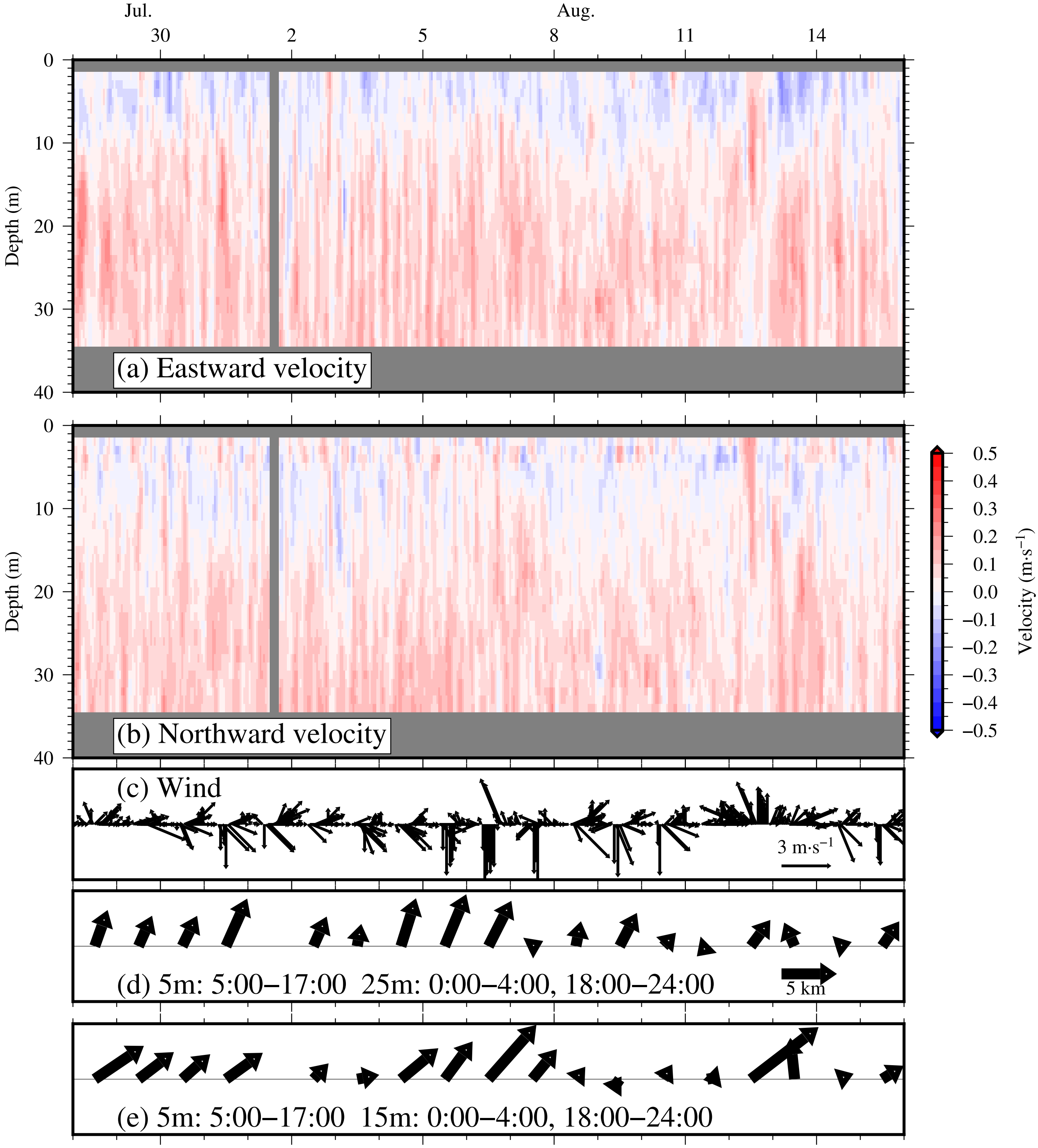

Fig.7 Aoki et al.

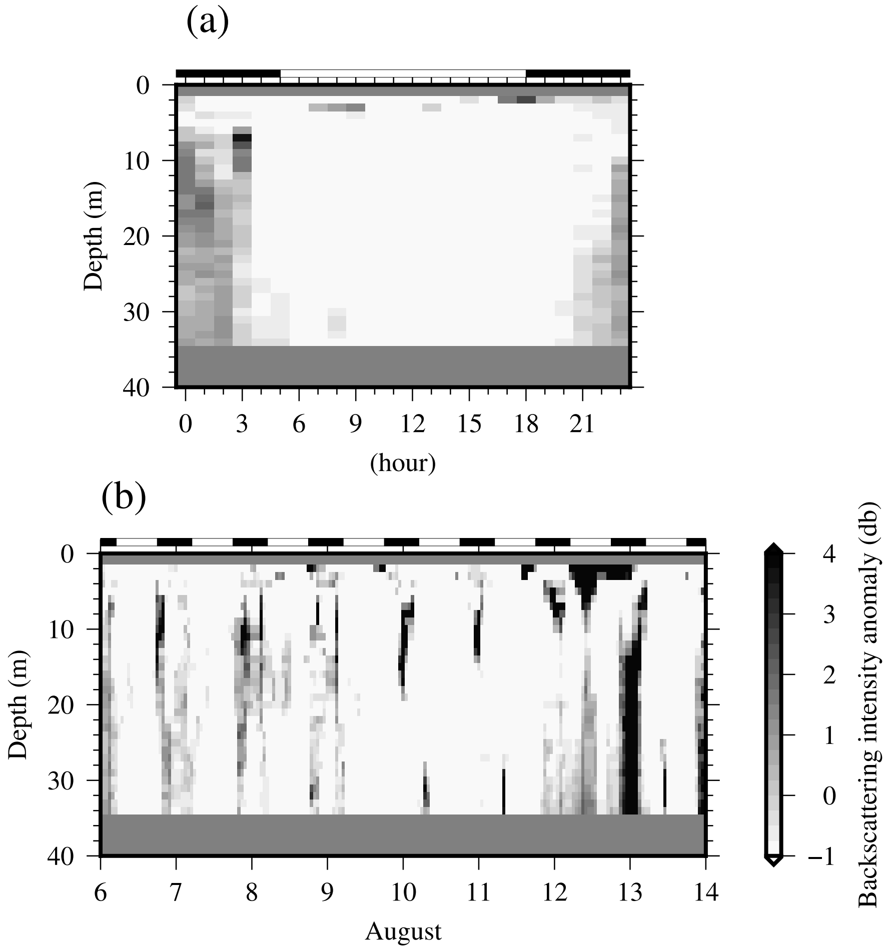

Fig.8 Aoki et al.